MODELING OF PLANAR VEHICLE DYNAMICS DURING GRADUAL TIRE DEFLATION

Alexander Brown, Sittikorn Lapapong, Kevin Swanson, Sean Brennan
Department of Mechanical and Nuclear Engineering, Penn State University
University Park, Pennsylvania, USA
aab5009@psu.edu

Abstract

A reasonable requirement for deployment of tire deflation devices is that a pursued suspect must be able to maneuver to a safe stop unless deadly force has been authorized. While a considerable body of literature concerning the dynamics of rapid tire blowouts exists, the more gradual tire deflation associated with TDDs or tires with minor punctures is seldom, if ever, addressed in experimental vehicle dynamics. This paper investigates the dynamics associated with slow tire deflation and presents a novel method for determining tire pressure by using direct tire radius measurements. During a tire deflation, the cornering stiffness of the tire changes with pressure, and so a method for determining cornering stiffness based on pressure is presented that fits a polynomial curve to experimental cornering stiffness data. Knowing the variable cornering stiffness enables the use of an all-integrator version of the planar bicycle model to model vehicle motion during a slow tire deflation. Experimental results show that yaw rate can be accurately predicted during a slow tire deflation based on these models.

1. INTRODUCTION

Tire deflation devices (TDDs) are the most commonly deployed high-speed police pursuit intervention technology. A reasonable requirement for deployment of pursuit intervention technologies is that a pursued suspect must be able to maneuver to a safe stop unless deadly force has been authorized. While a considerable body of literature concerning the dynamics of rapid tire blowouts exists, the more gradual tire deflation associated with TDDs or tires with minor punctures is seldom, if ever, addressed in experimental vehicle dynamics. Even so, vehicle behavior during a tire deflation caused by a small incidental puncture or police TDD deployment is important for designers of both roadways and police pursuit policies to understand.

This paper investigates the dynamics associated with a tire deflation instigated by a TDD deployment using simple first-order models of tire deflation, experimentally determined relationships between tire pressure and tire lateral dynamics, and a planar bicycle model approximation of the afflicted vehicle. Past research by Patwardhan et al. [1] [2] and Blythe et al. [3] has involved rapid tire blowout. The main assumption used in rapid tire blowout is that it is an adiabatic process, e.g. so fast that heat transfer is negligible. For deflations caused by small punctures, however, the blowout is gradual and heat transfer cannot be ignored. Additionally, past efforts investigate many effects of tire blowouts including effects on rolling resistance, suspension, and cornering stiffness. This paper focuses primarily on loss of cornering stiffness during slow deflations to predict vehicle yaw rate based on steering input.

Due to the high cost of research-grade wireless tire pressure sensors, the authors relied on indirect tire pressure monitoring for real- time measurements during experiments. The method used in this paper is simpler than the one used by Persson et al. [4] where data is obtained through a fusion of vibration dynamics and rolling wheel radius based off of wheel speeds. In this paper, pressure is found by a simple and direct measurement of wheel radius using an infra-red proximity sensor.

The remainder of this paper is organized as follows: Section two introduces the proposed model for tire pressure change after a TDD strike, and introduces a novel method of experimentally determining tire pressure indirectly. Section three outlines the changes in tire properties observed at varying tire pressures, and features experimental results of a deflation test juxtaposed against model predictions. Section four offers a conclusion summarizing the experimental and simulated results.

2. METHOD

2.1 Tire Deflation Model

To obtain a model of a slowly deflating tire, the inflated tire is modeled as a pneumatic capacitor with a known volume. The TDD strike is assumed to impinge an array of hollow TDD spikes into the tire, modeled as pneumatically resistive capillaries in series. The following ordinary differential equation is used to approximate the change in tire pressure after a TDD is encountered by a test vehicle. It is obtained by assuming that the deflation event is slow enough to be isothermal and the tire's volume is considered approximately constant during deflation.

$$\frac{dP_{tire}}{dt} = \frac{R*T*K_w}{v_{tire}*g} * (P_{tire}^2 - P_{atm}^2) \tag{1}$$

In this equation R is the universal gas constant, T is the ambient temperature in Kelvins, g is the gravitational acceleration constant, and υ_{tire} is the nominal tire volume. Here, K_w is an empirically derived fitting parameter describing a pneumatic resistance representative of an orifice corresponding to a particular type of TDD. Approximating a tire deflation this way is unique; modeling of deflation by Patwardhan and Tomizuka in [2] and other previous studies assumed an adiabatic pneumatic process consistent with the fast deflation rates of these studies. Heat transfer can safely be ignored during a fast tire blow-out, but not during deflations that can last tens of seconds where heat transfer is fast enough that an isothermal approximation is reasonable.

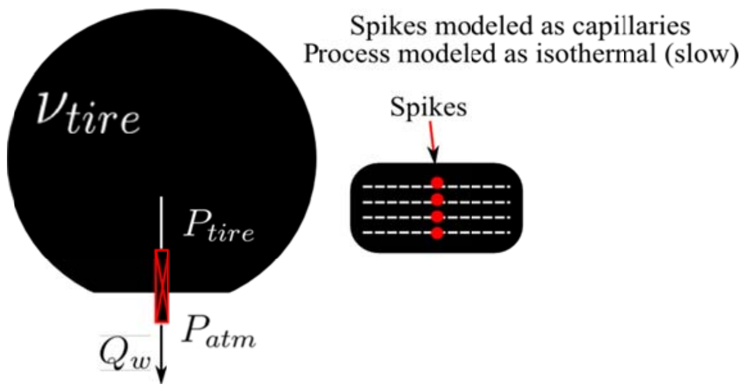

Figure 1: Physical Diagram for Tire Deflation Model

2.2 Relationship Between Wheel Center Height and Pressure

In these experiments tire pressure was not measured directly. Instead, a non-contact infra-red distance sensor mounted to stationary wheel encoders and aimed at the road surface provided wheel center height measurements at over 100Hz. Assuming a rectangular tire contact patch, a static force balance on the tire patch yields the following equation for tire pressure.

$$P_{tire} = \frac{W_{corner}}{w_{section}*L_{patch}} + P_{atm} \tag{2}$$

This pressure equation leads to the following equation for tire radius:

$$R_{eff=} R_{nom} * \cos(\sin^{-1}(\frac{W_{corner}}{2*P_{tire}*w_{section}*R_{nom}})) \tag{3}$$

where R_{nom} is the unladen tire radius at nominal tire pressure.

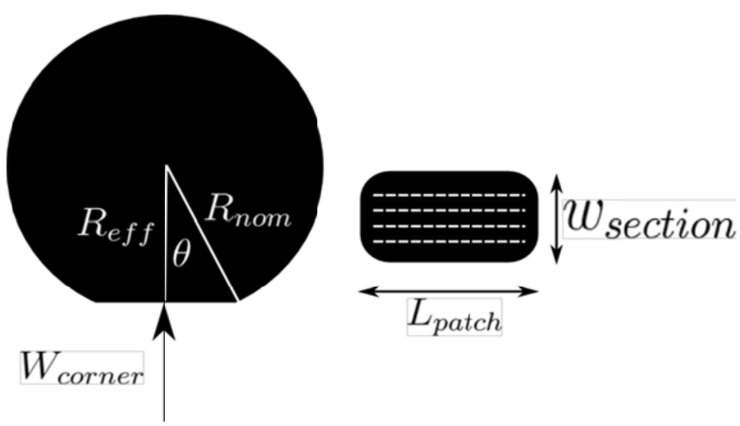

Figure 2: Physical Diagram for Radius Model

2.3 Experimental Model Verification and Simulations

In order to justify the relationship between wheel center height and tire pressure, an experiment was conducted to directly compare center height and tire pressure measurements. The tires were filled to 60 PSI and air was slowly released from the tire while data was simultaneously collected from the infra-red sensor, a ruler, and a tire pressure gage at 5 PSI intervals. Figure 3 below shows the quadratic fit equation for correlating infra-red sensor value to distance in inches in the local measured range. Figure 4 shows the correlation between the measured height at each pressure using both the ruler and IR sensor, along with the height calculated from the effective radius equation in section 2.2.

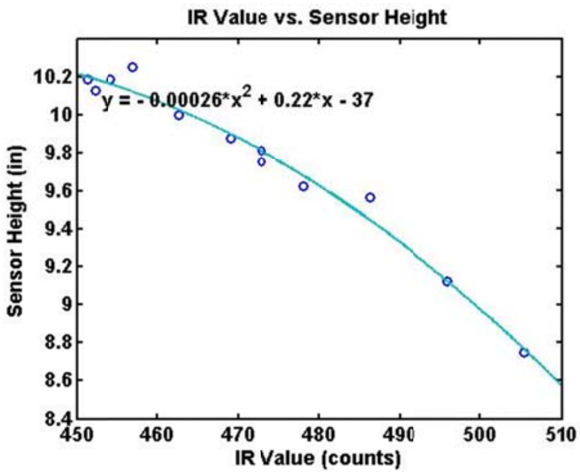

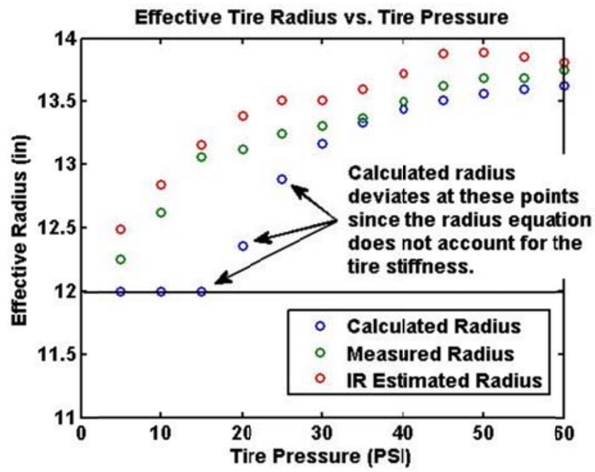

lated

Figure 4 shows a close correlation between measured and calculated radius at higher pressures, but the fit diverges at lower pressures. The lower limit of this divergence is bounded at 12 inches based on the rim size of the tire plus the compressed rubber of the completely deflated tire. The more rapid decrease in radius for the radius predicted by equation (3) could be explained by the fact that the radius equation does not account for tire sidewall stiffness. Additionally, as the tire deflates, the shape of the contact patch may vary and a constant width rectangle may not be the best approximation. Even though the curves diverge at low pressures, this equation is useful for its close correlation at transitional pressures between normal driving and total deflation.

The tunable parameter *K* for capillary resistance of TDD spikes was fit to a representative test of one brand of TDD on normal passenger tires. Simulations were used to predict measured tire radius as a function of time after a TDD strike. To investigate whether the model generalized well across tire volumes, a low-profile tire was also deflated, and the results of effective radius simulations were compared to actual measured tire radius during testing. Both simulations use a K value of $1.25\text{x}10^{-6}$ m^3-sec/kg since the same TDD is used in each test. The results are shown below.

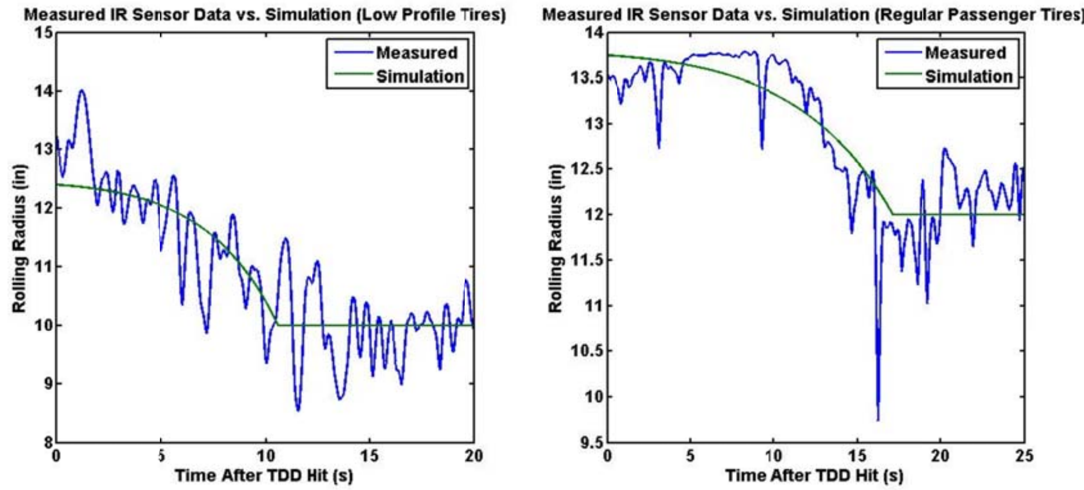

Figure 5: Simulated and Measured Tire Radius During Deflation of Low Profile and Regular Passenger Tires

The authors found that the model predicts wheel radius well across tire volumes and for several different TDD designs.

3. EFFECT OF TIRE DEFLATION ON VEHICLE DYNAMICS

3.1 Relating Tire Pressure to Cornering Stiffness

In order to assess changes in lateral vehicle dynamics associated with gradual tire deflation, an accurate model for tire cornering stiffness as a function of tire pressure is vital. A series of skidpad-based cornering stiffness measurements was conducted at Penn State's Larson Transportation Institute 20-meter radius skidpad at tire pressures of 60, 50, 40, 30, 20, and 10 psi. These experiments yielded measurements of cornering stiffness representing averages of tire lateral force required to maintain the circular path divided by measured slip angles, which were obtained using a Honeywell HG1700 ordnance-grade inertial measurement unit paired with a 100Hz RTK-enabled Novatel Span 4 GPS system. The results of these experiments can be seen below:

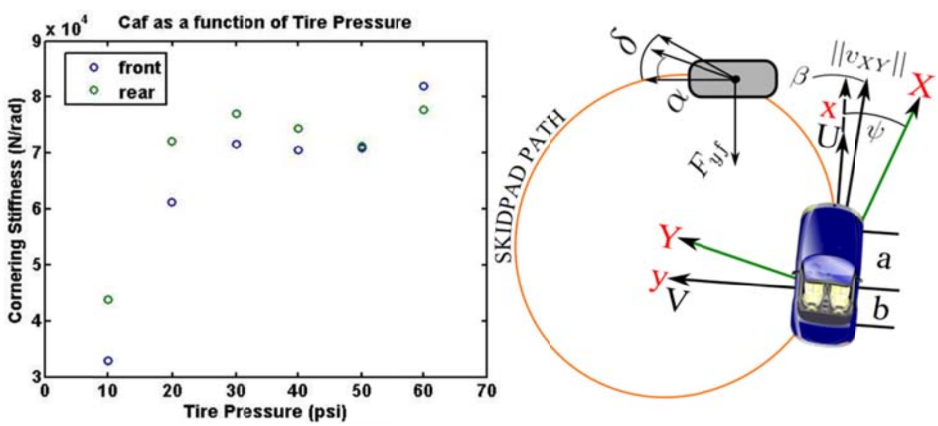

Figure 6: Cornering Stiffness vs. Tire Pressure as Measured on a 20 Meter Skidpad

The results show a third-order polynomial relationship between tire pressure and cornering stiffness seen below for both the front and rear tires, respectively.

$$C_{\propto f} = 1.7 * {P_{tire}}^{3} - 200 * {P_{tire}}^{2} + 7700 * P_{tire} - 26000 \quad (4a)$$

$$C_{\propto r} = 1.7 * {P_{tire}}^{3} - 210 * {P_{tire}}^{2} + 7700 * P_{tire} - 14000 \quad (4b)$$

3.2 Lane Change Maneuver

An all-integrator version of the planar bicycle model yielded vehicle yaw for a double lane change maneuver. The equations for this model can be seen below. To verify model fit for maneuvers without tire deflation, the simulation was run with constant values of front and rear cornering stiffness.

$$\dot{V} = \left(\frac{C_{\propto f}+C_{\propto r}}{m*U}\right)*V+\left(\frac{a*C_{\propto f}-b*C_{\propto r}}{m*U}-U\right)*r-\frac{C_{\propto f}}{m}*\delta_f \quad (5a)$$

$$\dot{r} = \left(\frac{a*C_{\propto f}-b*C_{\propto r}}{I_z*U}\right)*V+\left(\frac{a^2*C_{\propto f}+b^2*C_{\propto r}}{I_z*U}\right)*r-\frac{a*C_{\propto f}}{I_z}*\delta_f \quad (5b)$$

Model agreement in cases where no deflation takes place is shown in Figure 7.

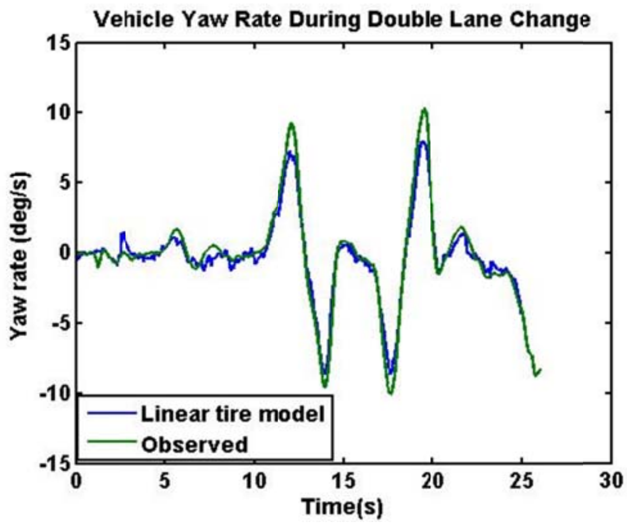

Figure 7: Vehicle Yaw Rate During Double Lane Change

To assess the validity of the tire deflation model and its relationship to tire cornering stiffness, the vehicle's yaw rate was simulated for a lane change during front tire deflation using equations (5a) and (5b). In this simulated system's tire model, cornering stiffness varied with pressure as predicted by the tire deflation equations (4a) and (4b). Model agreement for vehicle yaw rate is shown below for a mild lane change performed during one deflation test while the test vehicle decelerated gradually. The use of gradual deceleration allowed for longitudinal tire dynamics to be neglected.

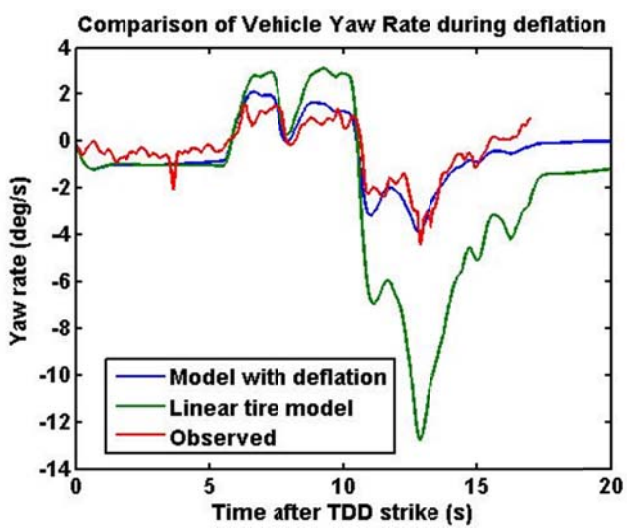

Figure 8: Comparison of Vehicle Yaw Rate During Deflation

Figure 8 shows a close correlation between the simulated yaw rate and the observed yaw rate during a deflation event, which confirms that that the yaw rate gain changes significantly with deflation. The observed changes in yaw rate gain are important because there is ongoing work, for example that of Persson et al. [4], to predict tire pressure by fusing yaw rate measurements derived from encoder data to those obtained with a gyroscope using a kinematic EKF. This work suggests that estimation of tire inflation from yaw-rate creates a feedback loop, since tire pressure significantly affects yaw rate for situations of interest such as low tire inflation.

The agreement over time also gives confidence in the approximations for deflation dynamics and resulting influence on chassis dynamics. If the pneumatic resistance values were significantly in error, the gradual change in yaw-rate behavior would not be captured. And given that the results give good agreement across many different tires (not shown), this suggests that the fit is indeed capturing both pressure and volume effects and is not simply an artifact of fitting the pneumatic resistance value to a specific tire.

Finally, the observed changes in dynamics confirms that one can maneuver a vehicle safely after a TDD impact, as long as the required maneuvering does not require significant steering (yaw rate). Again, this agrees with intuition as most TDD impacts deflate the front tires primarily, resulting in a severely understeer vehicle which has limited maneuverability.

4. CONCLUSIONS

A main goal of this work was to predict a vehicle’s handling capability during an induced tire deflation. First, an indirect but simple method was presented to determine tire radius, and this radius was correlated to tire pressure. Experiments were then conducted to relate cornering stiffness to tire pressures below nominal values. Both trends were used to obtain the tire’s corning stiffness from a measurement of effective tire radius. To predict the vehicle dynamics, a tire deflation model was developed by assuming constant air temperature inside a tire during slow deflation. This deflation model was used to estimate time-varying cornering stiffness, estimates which were then used in a parameter-varying version of the planar bicycle model to predict vehicle motion. The simulated vehicle dynamics inclusive of tire deflation match closely with the experimental data, whereas the constant-parameter form of the planar bicycle model does not.

Such results might allow a higher-fidelity tire pressure monitoring scheme based on yaw rate measurements. This remains for future work.

5. ACKNOWLEGEMENTS

Portions of this work were conducted under the support of the National Institute of Justice whose purchase of TDD devices and many dozens of sets of tires for testing is greatly appreciated.

References

[1] S. Patwardhan and M. Tomizuka: *Experiments of Tire Blow-out Effects and Hazard Reduction Control for Automated Vehicle Lateral Control System.* Baltimore, MD : s.n., 1994. Proceedings of the American Control Conference. pp. 1207-1209.

[2] S. Patwardhan, H.-S. Tan, and M. Tomizuka.: *Experimental Results of a Tire-Burst Controller for AHS.* 11, s.l. : Control Eng. Practice, 1997, Vol. 5.

[3] W. Blythe, T. Day, and W. Grimes: 3-*Dimensional Simulation of Vehicle Response to Tire Blow-outs.* Detroit, Michigan : SAE International, 1998.

[4] N. Persson, F. Gustafsson, and M. Drevo: *Indirect Tire Pressure Monitoring Using Sensor Fusion.* SAE International, 2002. 2002-01-1250.